



**Fluid interface-mediated nanoparticle membrane as electrochemical sensor**

Journal:	<i>RSC Advances</i>
Manuscript ID:	RA-COM-10-2014-012149.R1
Article Type:	Communication
Date Submitted by the Author:	06-Nov-2014
Complete List of Authors:	Ali, Mohammed; Assam University, Department of Chemistry Barman, Koushik; Assam University, Department of Chemistry Sk, Jasimuddin; Assam University, Chemistry Ghosh, Sujit; Assam University, Department of Chemistry

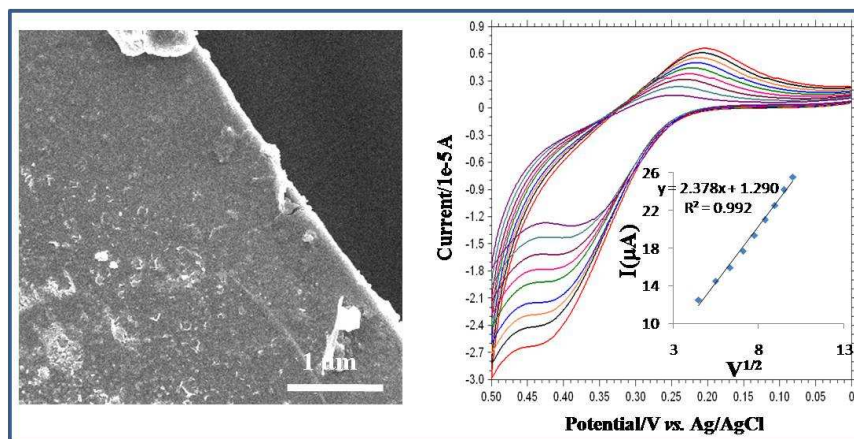
## Table of Contents

---

### Nanoparticle-decorated ultra-thin membrane as electrochemical sensor

Mohammed Ali, Koushik Barman, Sk. Jasimuddin and Sujit Kumar Ghosh

Poly(ethyleneglycol)-stabilised magnetic  $\text{Fe}_3\text{O}_4$  nanoparticles decorated ultra-thin membrane has been devised at the water/ $\text{CCl}_4$  interface by ligand cross-linking with terephthaloyl chloride and the membrane was exploited as **electrochemical sensor for the detection of L-Dopa** up to nanomolar concentration.



Cite this: DOI: 10.1039/c0xx00000x

www.rsc.org/xxxxxx

## COMMUNICATION

# Fluid interface-mediated nanoparticle membrane as electrochemical sensor

Mohammed Ali, Koushik Barman, Sk. Jasimuddin and Sujit Kumar Ghosh\*

Received (in XXX, XXX) Xth XXXXXXXXX 20XX, Accepted Xth XXXXXXXXX 20XX

DOI: 10.1039/b000000x

**Poly(ethyleneglycol) (PEG-13)-stabilised magnetic Fe<sub>3</sub>O<sub>4</sub> nanoparticles decorated ultra-thin membrane has been devised at the water/chloroform interface by ligand cross-linking between pendant hydroxyl groups of PEG with terephthaloyl chloride. Such robust nanoparticle-decorated membrane has been employed as electrochemical sensor for the detection of L-Dopa up to nanomolar concentration.**

## 1. Introduction

The fabrication of membranes via self-assembly of nanoscale materials is of interest for delivery vessels, size-selective separation and purification, controlled-release materials, sensors and catalysts, scaffolds for tissue engineering, low dielectric constant materials for microelectronic devices, antireflective coatings and proton exchange membranes for polymer electrolyte membrane fuel cells etc.<sup>1-4</sup> Recently, nanocrystalline iron oxides, composites and related materials have received special attention due to their viability as a platform for electrochemical, magnetic, and chemical biosensors.<sup>5,6</sup> While many kinds of nanoparticles, such as, metal, metal oxide and semiconductor nanoparticles have been used for constructing electrochemical sensors and biosensors, these nanoparticles play different roles in different sensing systems.<sup>7</sup> Since, the electrochemical detection is based on the current changes by modifying the electrode surface covered with a thin layer of particles due to the presence of chemical components of the reacting system, therefore, it has to make sure that, all the particles should be well-connected to each other so that the impulse could be transmitted throughout. Based on these conceptives, a robust and ultrathin membrane made up of nanoparticles could be an effective choice for electrochemical sensing applications rather than, simply, attaching a layer of particles on the electrode surface. Such membrane-based electrochemical sensor is not only effective but also more sensitive than the conventional particle-based sensors,<sup>8</sup> while the fabrication of such membrane and draping it onto the electrode surface remain challenging.

L-Dopa is the immediate precursor of the neurotransmitter dopamine, that plays a very crucial role in the functioning of the central nervous, cardiovascular, renal, and hormonal systems, as

well as in drug addiction and Parkinson's disease.<sup>9</sup> Thus, it becomes imperative for neuro and analytical scientists to find out a means to detect the presence of L-Dopa in human body up to trace amount.<sup>10</sup> Several techniques for the detection of L-Dopa have been described in the literature, including, flow injection method,<sup>11</sup> fluorescence spectroscopy,<sup>12</sup> cyclic voltammetry<sup>13,14</sup> and so on. While different types of membranes *e. g.*, nafion membranes,<sup>15</sup> enzyme collagen membranes,<sup>16</sup> bilayer lipid membranes,<sup>17</sup> gallium arsenide electrodes functionalised with supported membranes<sup>18</sup> have, conventionally, been used for electrochemical sensing and nanoparticle-decorated ultrathin membrane have been employed to study their permeability and elasticity,<sup>19</sup> nanofiltration,<sup>20</sup> triggered release from liposomes,<sup>21</sup> targeted transfection<sup>22</sup> and so on; we have been interested to exploit nanoparticle-membrane as electrochemical sensor. In this communication, we have reported the fabrication of Fe<sub>3</sub>O<sub>4</sub> nanoparticle-decorated ultrathin membrane at the water/chloroform interface by terephthaloyl chloride and the membrane has been employed for electrochemical detection of L-Dopa up to nanomolar concentration.

## 2. Experimental

### 2.1 Reagents and instruments

All the reagents used were of analytical reagent grade. L-Dopa and phosphoric acid (Sigma Aldrich), PEG-13 (Broad Pharm, USA), anhydrous FeCl<sub>3</sub> and ammonium ferrous sulphate (Merck, India) were used without further purification. Chloroform and ammonia (S. D Fine Chemicals, India) and sodium perchlorate (Sisco Research Laboratories, India) were used as received. An aliquot of 0.1 M phosphate buffer saline (PBS) was prepared by mixing of equimolar solution of phosphoric acid and sodium perchlorate followed by dropwise addition of sodium hydroxide. Double distilled water was used throughout the course of the experiment. The temperature was 298±1 K for all experiments.

The membrane was observed by optical microscope (Olympus BX 61) equipped with a high resolution DP70 digital charge coupled device (CCD) camera and images were processed using Aldus Photostyler 3.0 software. Scanning electron micrographs were recorded by using JEOL JSM-6360 instrument equipped with a field emission cathode with a lateral resolution of approximately 3 nm and acceleration voltage 3 kV after sputtering the sample on silicon wafer with carbon (approx. 65 nm). Thin films were prepared by drop-coating the membrane

Department of Chemistry, Assam University, Silchar-788011,  
India

E-mail: sujit.kumar.ghosh@aus.ac.in

from water/chloroform interface and transferred onto silicon wafer with the help of a micropipette. Transmission electron microscopy was carried out on a JEOL JEM-2100 microscope with a magnification of 200 kV. Samples were prepared by placing a drop of solution on a carbon coated copper grid and dried overnight under vacuum. High-resolution transmission electron micrographs and selected area electron diffraction pattern were obtained using the same microscope. Fourier transform infrared (FTIR) spectra were recorded in the form of pressed KBr pallets in the range (400–4000  $\text{cm}^{-1}$ ) in Shimadzu-FTIR Prestige-21 spectrophotometer. Electrochemical measurements were performed by a CHI-660C electrochemical workstation. An Ag/AgCl electrode (in 3.0 M KCl) and a Pt wire were used as reference and auxiliary electrodes, respectively. Catalytic reactions were performed by the immobilized nanoparticles or nanocomposites over a 4-aminothiophenol monolayer modified gold working electrode where 0.1 M phosphate buffer saline (pH~7.5) was used as electrolyte and the scan rate was 100 mV/s.

### Synthesis of $\text{Fe}_3\text{O}_4$ nanoparticles

Polyethylene glycol (PEG-13)-stabilised iron oxide nanoparticles were synthesised by modification of the procedure reported by Gillich et al.<sup>23</sup> In a typical synthesis, 1.99 g (0.01 mol)  $(\text{NH}_4)_2\text{Fe}(\text{SO}_4)_2 \cdot 6\text{H}_2\text{O}$  and 5.41 g (0.02 mol)  $\text{FeCl}_3 \cdot 6\text{H}_2\text{O}$  were dissolved in 50 mL distilled water in a beaker so that the molar ratio of  $\text{Fe}^{2+} : \text{Fe}^{3+} = 1 : 2$ . In a separate beaker, an aqueous  $\text{NH}_4\text{OH}$  (30% v/v) solution (1.5 M) was prepared. Then, polyethylene glycol (0.1 M) was added at a ratio of 1 : 10 to both the above solutions to get precursor solutions I and II respectively. After that, precursor solution II was added to solution I dropwise under stirring condition at 40  $^\circ\text{C}$ ; just after mixing the solutions, colour of the solution changes from light brown to black indicating the formation of  $\text{Fe}_3\text{O}_4$  nanoparticles. The stirring was continued for another 45 min and the solution was cooled to room temperature. The precipitate so-obtained was washed thrice by centrifugation and redispersed in distilled water. The particles are spherical or nearly spherical and the size of the particles was found to be  $5 \pm 0.5$  nm.

### Synthesis of membrane

Ultrathin membrane made up of PEG-coated  $\text{Fe}_3\text{O}_4$  nanoparticles were synthesised at water/chloroform interface by intermolecular polymerization between pendant  $-\text{OH}$  groups of PEG anchored onto  $\text{Fe}_3\text{O}_4$  nanoparticles surfaces with the help of terephthaloyl chloride (TC), a well-known ligand cross-linker. In a typical method, 2 mL of  $\text{Fe}_3\text{O}_4$  hydrosol (0.25 mM) was taken in a test tube and equal volume of chloroform containing small amount of terephthaloyl chloride was mixed and shaken vigorously. After about 2 min, the mixture was allowed to settle and after few moments, the formation of a membrane has been observed at the interface.

## 3. Results and discussion

The structure and morphology of the membrane has been characterised by optical microscopy, scanning electron microscopy (SEM), transmission electron microscopy (TEM) and

high resolution transmission electron microscopic images (HRTEM) as shown in Fig. 1. Panel a shows the optical microscope image of the as-prepared membrane. The membrane so-formed at the interface was collected by micropipette and kept suspended in chloroform in the cavity of a glass slide. An ultrathin membrane can, clearly, be observed; the ridges on the

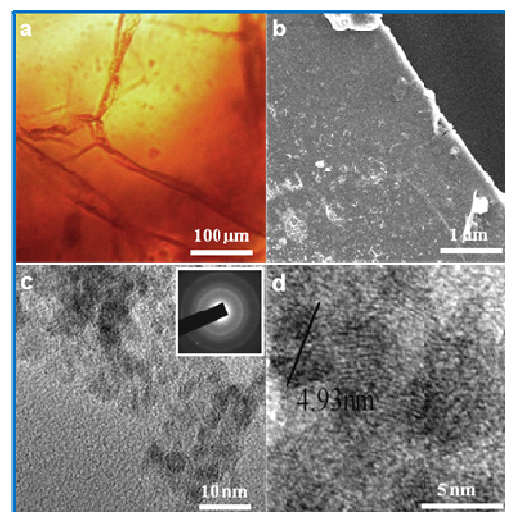


**Fig. 1.** (a) Optical micrograph, (b) scanning electron micrograph, (c) transmission electron micrograph and (d) high resolution transmission electron micrograph of the  $\text{Fe}_3\text{O}_4$  nanoparticle-decorated membrane. Inset in panel c shows the selected area electron diffraction pattern of the membrane.

membrane arises during the transfer of the membrane by micropipette on the glass slide, which, in turn, support robustness of the membrane.<sup>19</sup> Typical SEM image of the membrane (panel b) exhibit the formation of an intact and robust membrane at water/chloroform interface.<sup>22</sup> Panel c is the representative transmission electron micrograph of the membrane which shows compact and regular monolayer arrangement of the nanoparticles in the membrane.<sup>24</sup> The selected area electron diffraction (SAED) pattern shown in the inset exhibits five distinct diffraction rings of (220), (311), (420), (511) and (440) confirmed a typical magnetite crystalline structure.<sup>25</sup> Panel d is the high resolution TEM image of the membrane which, further, confirms two dimensional ordering of the  $\text{Fe}_3\text{O}_4$  nanoparticles in the membrane.<sup>26</sup>

The ligand cross-linking between the chain-end hydroxyl groups of PEG via terephthaloyl chloride has been monitored by FTIR spectroscopy. Fig. 2 shows the overlaid FTIR spectra of PEG-13 stabilised  $\text{Fe}_3\text{O}_4$  nanoparticles (trace a) and nanoparticle-decorated membrane formed after cross-linking (trace b). It is observed that, the peaks at ca. 3360 and 3420  $\text{cm}^{-1}$  corresponding to  $-\text{O}-\text{H}$  stretching is disappeared indicating successful cross-linking between hydroxyl groups of PEG with the acyl chloride moiety of the terephthaloyl chloride molecules.<sup>27</sup>

It is well-established in the literature that ultrasmall particles strongly segregate to the interface of immiscible fluids, driven by a reduction of interfacial energy.<sup>1-3</sup> When such interfacial assembly of nanoparticles takes place in a 2D interface (a flat surface), thin films of nanoparticles could be produced *in-situ* at interfaces between immiscible fluids. Such membranous structure

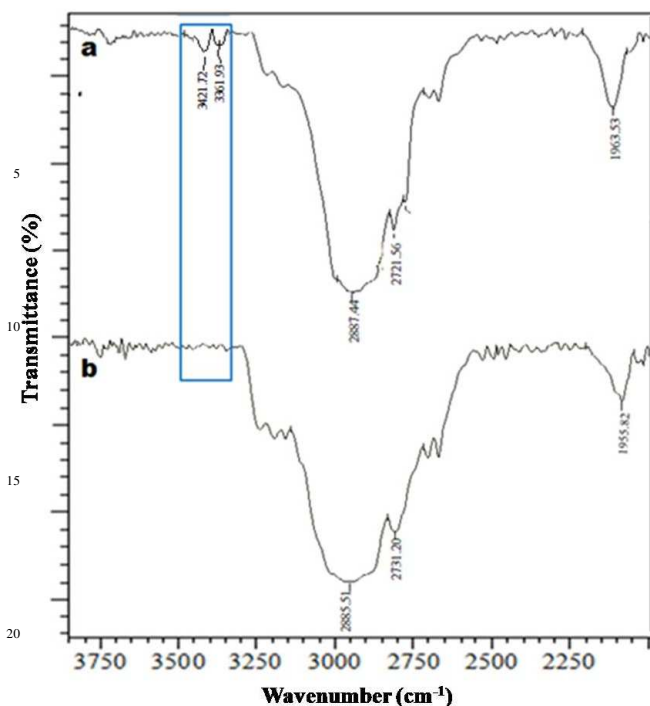


**Fig. 2.** FTIR spectra of PEG-stabilised  $\text{Fe}_3\text{O}_4$  nanoparticles (a) before and (b) after cross-linking.

may be less stable, but when the nanoparticles used in these interfacial assemblies are decorated with functional ligands, the assemblies can be stabilized and transformed into robust materials by performing chemistry on the functional groups contained within the ligand structure.<sup>1,3</sup> In this experiment, the PEG-13 stabilised  $\text{Fe}_3\text{O}_4$  nanoparticle-decorated membrane at the water/chloroform interface has been stabilized by cross-linking the chain-end hydroxyl groups of PEG with two acyl chloride moieties of terephthaloyl chloride, as represented in Scheme 1.

The magnetism of the membrane acquired, by virtue, of its magnetic nanoparticles as building blocks, was investigated by applying an external magnetic field. (Fig. 3). A homogenous uniform membrane with over a large area ( $\sim 55.4 \text{ cm}^2$ ) is seen in the absence of the magnet (panel a). However, the membrane becomes folded towards a bar magnet when it is placed nearby and unfolded when the magnet bar is taken away. The membrane folding and unfolding is observed even up to ten cycles of operations pointing out the mechanical robustness of the liposomes through magnetic actuation of superparamagnetic iron constituted of cross-linked ultrasmall nanoparticles. Amstad et

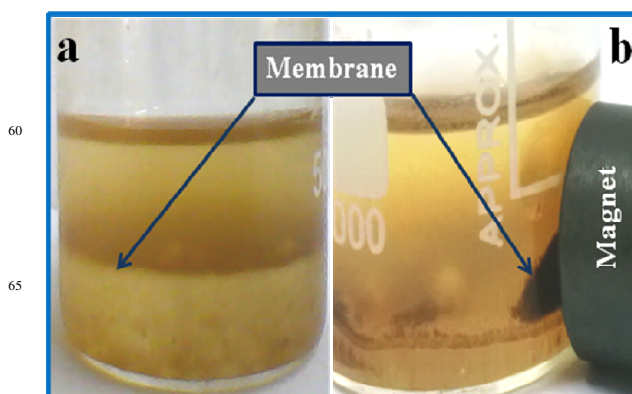
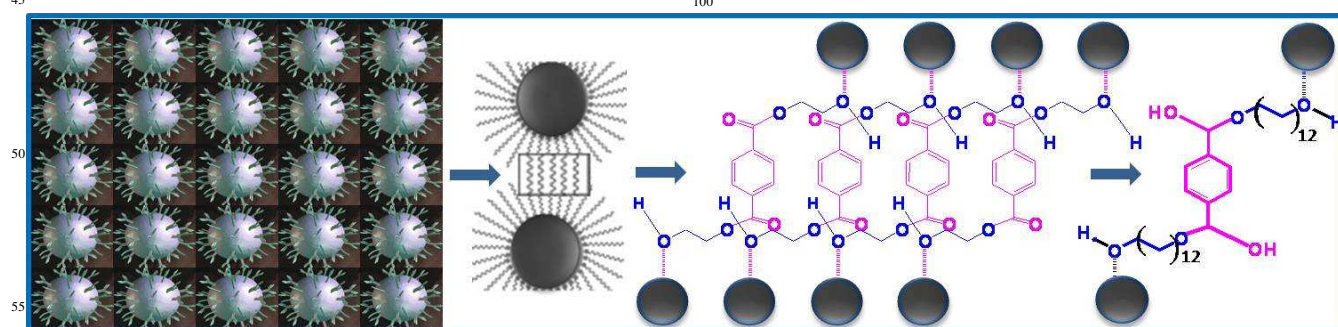


**Fig. 3.** Response of the nanoparticle-decorated ultrathin membrane in the (a) absence and (b) presence of a bar magnet

al.<sup>21</sup> have demonstrated triggered release from reversibility of oxide nanoparticle containing membranes. Therefore, magneto-responsibility of the membrane could be exploited in the near future for the development of efficient drug carriers that can deliver anti-cancer agents specifically into cancerous tissues exposed to a magnetic field.<sup>1,4</sup>

Now, the nanoparticle-decorated ultrathin membrane was employed as an electrochemical sensor for the determination of L-Dopa upto nanomolar concentration (Fig. 4). The modification of the gold electrode with the membrane and its electrochemical characterisation are described in ESI 1. A study of electrocatalytic oxidation of L-Dopa at different pH (ESI 2) indicates that the interaction between membrane-modified gold electrode and L-Dopa is optimum at pH 7.0. Panel a shows the cyclic voltammogram of 1.0 mM L-Dopa in 0.1 M PBS (pH  $\sim$  7.0) on bare and membrane-modified gold electrode (red curve). The appearance of a pair of weak redox peak was observed with a peak-to-peak separation,  $\Delta E_p = 230 \text{ mV}$  on the bare gold electrode. However, a well-defined irreversible redox wave ( $\Delta E_p = 188 \text{ mV}$ ) was seen on the modified electrode. It is noted that the anodic peak potential shifts negatively (26 mV) and the anodic peak current is higher (15  $\mu\text{A}$ ) in comparison with the bare electrode, which suggests that the membrane-modified gold electrode shows electrocatalytic oxidation of L-Dopa ( $\text{L-Dopa} + 2\text{H}_2\text{O} \rightarrow \text{Dopaquinone} + 4\text{H}^+ + 4\text{e}^-$ ). The transfer of four electrons for L-Dopa oxidation was confirmed by comparing the current height with the  $[\text{Fe}(\text{CN})_6]^{3-/4-}$  redox couple under similar measurement conditions.<sup>28</sup> The scan rate dependence of oxidation current of L-Dopa is proportional to the square root of the scan rate indicating that the oxidation is diffusion-controlled.<sup>29</sup> Panel b



**Scheme 1.** Schematic presentation of formation of nanoparticle-decorated membrane by cross-linking of chain end hydroxyl groups of PEG with acyl chloride moiety of terephthaloyl chloride via ester linkage formation.

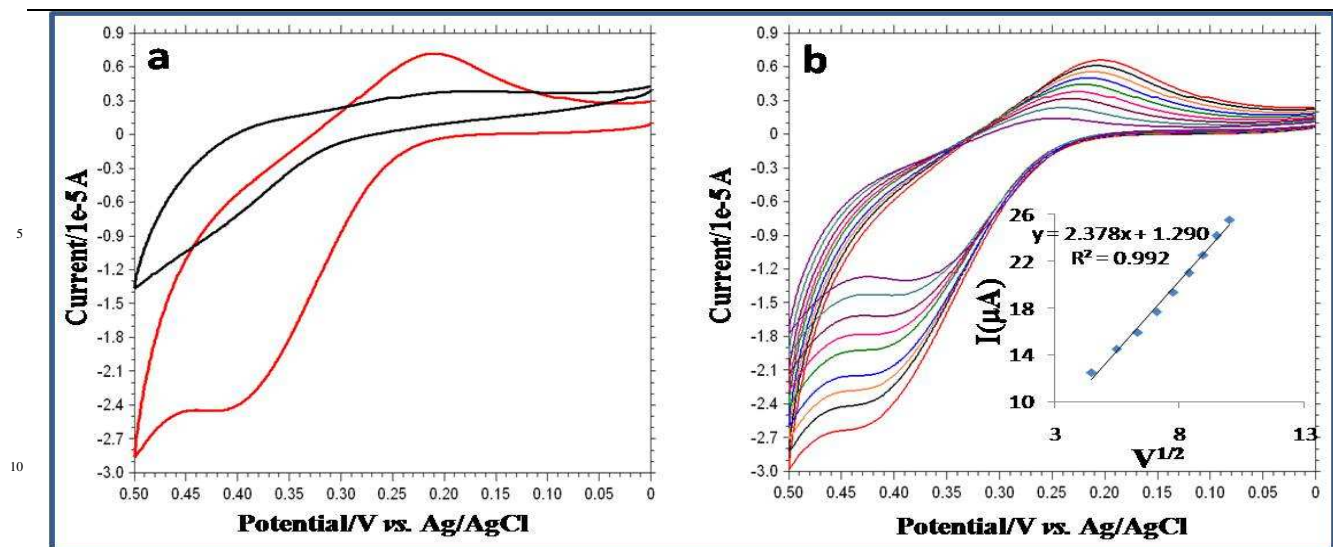


**Fig. 4.** (a) Cyclic voltammogram of 1.0 mM L-Dopa (at pH=7.0) at bare (black curve), and membrane-modified gold electrode (red curve); and (b) cyclic voltammetry of L-Dopa at different scan rate at membrane-modified gold electrode.

shows the cyclic voltammetric responses of the membrane-modified electrode for L-Dopa at different scan rate. Inset shows a plot of oxidation current with increase in concentration of L-Dopa. It is seen that, the oxidation current of L-Dopa increases, linearly, with increase in concentration in the range of 1- 4.5  $\mu\text{M}$ . The concentration of L-Dopa could be determined in the range 0.05 – 10  $\mu\text{M}$  and the limit of detection (LOD, an average of three determinations) was obtained as 9.5 nM using equation  $3\sigma/m$ , where,  $\sigma$  is the standard deviation of the measurement and  $m$  is the slope of the calibration curve,  $I_p (\mu\text{A}) = 0.122 C (\mu\text{M}) + 6.608$  and  $R^2 = 0.996$ . A comparative account of the sensing capabilities for the determination of L-Dopa in the presence of different materials and methods is presented in ESI 3. Moreover, it is seen that nanoparticle-decorated membrane is able to determine L-Dopa and ascorbic acid in binary mixtures of the compounds, linearly, in an appreciable concentration range (ESI 4). Therefore, it could be inferred that, the nanoparticle-decorated membrane could, even, be exploited as an electrochemical sensor for simultaneous determination of L-Dopa and ascorbic acid in a binary mixture of the compounds.

#### 4. Conclusion

In summary, water/chloroform interface has been exploited as a viable platform for the fabrication of  $\text{Fe}_3\text{O}_4$  nanoparticle-decorated robust, ultrathin membrane by cross-linking the chain-end hydroxyl groups of PEG ligands attached onto nanoparticle surface with the help of terephthaloyl chloride as the ligand cross-linker. This nanoparticle-decorated ultrathin membrane has been, successfully, employed for electrochemical detection of L-Dopa (and also L-Dopa and ascorbic acid simultaneously) up to nanomolar level concentrations. The membrane could be manipulated in the near future using external magnetic field, providing a convenient and gentle means to utilise as efficient delivery vehicles for various therapeutic agents, particularly, in cancer therapy.

**Acknowledgements.** We gratefully acknowledge financial support from DST, New Delhi (Project No.: SR/FT/CS-68/2010).

**Supporting Information.** Instrumentation and experimental details, cyclic voltammetry and differential pulse voltammetry. This material is available free of charge at <http://www.rsc.org>.

#### Notes and references

1. D. Wang, H. Möhwald, *H. J. Mater. Chem.*, 2004, **14**, 459–468.
2. W. H. Binder, *Angew. Chem. Int. Ed.*, 2005, **44**, 5172–5175.
3. A. Böker, J. He, T. Emrick, T. P. Russell, *Soft Matter*, 2007, **3**, 1231–1248.
4. P. van Rijn, M. Tutus, C. Kathrein, L. Zhu, M. Wessling, U. Schwaneberg, A. Böker, *Chem. Soc. Rev.*, 2013, **42**, 6578–6592.
5. S. Laurent, D. Forge, M. Port, A. Roch, C. Robic, L. Vander Elst, R. N. Muller, *Chem. Rev.*, 2008, **108**, 2064–2110.
6. V. Urbanova, M. Magro, A. Gedanken, D. Baratella, F. Vianello, R. Zboril, *Chem. Mater.*, 2014, doi: 10.1021/cm500364x.
7. M. Pumera In *Nanomaterials in electrochemical sensing and biosensing*, 2013, CRC Press, Boca Raton, USA.
8. X. Luo, A. Morrin, A. J. Killard, M. R. Smyth, *Electroanalysis*, 2006, **18**, 319–326.
9. P. Damier, E. C. Hirsch, Y. Agid, A. M. Graybiel, *Brain*, 1999, **122**, 1437–1448.
10. B. J. Venton, R. M. Wightman, *Anal. Chem.*, 2003, **224**, 414 A–421 A.
11. M. F. S. Teixeira, L. H. Marcolino-Júnior, O. Fatibello-Filho, E. R. Dockal Márcio, F. Bergamini, *Sens. Actu. B*, 2007, **122**, 549–555.
12. A. Coskun, E. U. Akkaya, *Org. Lett.*, 2004, **6**, 3107–3109.
13. F. R. Leite, C. M. Maroneze, A. B. de Oliveira, W. T. dos Santos, F. S. Damos, C. Silva Luz Rde, *Bioelectrochem.*, 2012, **86**, 22–29.
14. X. Yan, D. Pan, H. Wang, X. Bo, L. Guo, *J. Electroanal. Chem.*, 2011, **663**, 36–42.
15. R. C. Mercado, F. Moussy, *Biosensors & Bioelectronics*, 1998, **13**, 133–145.

- 
16. D. R. Thevenot , R. Sternberg , P. R. Coulet , J. Laurent, D. C. Gautheron *Anal. Chem.*, 1979, **51**, 96–100.
  17. D. P. Nikolelis, U. J. Krull, *Electroanalysis*, 1993, **5**, 539–545.
  18. D. Gassull, A. Ulman, M. Grunze, M. Tanaka, *J. Phys. Chem. B*, 2008, **112**, 5736-5741.
  19. Y. Lin, H. Skaff, A. Böker, A. D. Dinsmore, T. Emrick, T. P. Russell, *J. Am. Chem. Soc.*, 2003, **125**, 12690-12691.
  20. J. He, X. –M. Lin, H. Chan, L. Vukovic, P. Kräl, H. M. Jaeger, *Nano Lett.*, 2011, **11**, 2430–2435.
  21. E. Amstad, J. Kohlbrecher, E. Müller, T. Schweizer, M. Textor, E. Reimhult, *Nano Lett.*, 2011, **11**, 1664-1670.
  22. M. Delcea, N. Sternberg, A. M. Yashchenok, R. Georgieeva, H. Bäuml, H. Möhwald, A. G. Skirtach, *ACS Nano*, 2012, **6**, 4169-4180.
  23. T. Gillich, C. Acikgöz , L. Isa , A. D. Schlüter N. D. Spencer, M. Textor, *ACS Nano* 2013, **7**, 316-329.
  24. M. Ali , S. Bora, S. K. Ghosh, *Langmuir*, 2014, **30**, 10449–10455.
  25. R. M. Cornell, U. Schwertmann, *The Iron Oxides*, 2nd edn., VCH:Weinheim, 2003.
  26. B. Samanta, D. Patra, C. Subramani, Y. Ofir, G. Yesibug, A. Sanyal, V. M. Rotello, *Small*, 2009, **5**, 685-688.
  27. S. T. Hussain, M. Iqbal, M. Mazhar, *J. Nanopart. Res.*, 2009, **11**, 1383–1391.
  28. J. P. E. Spencer, P. Jenner, S. E. Daniel, A. J. Lees, D. C. Marsden, B. Halliwell, *J. Neurochem.* 1998, **71**, 2112-2122.
  29. M. Mazloum-Ardakani, M. Yavari, M. Ali Sheikh-Mohseni, B. F. Mirjalili, *Catal. Sci. Technol.*, 2013, **3**, 2634-2638.